METABOLISM

Anti-obesity effects of GIPR antagonists alone and in combination with GLP-1R agonists in preclinical models

Elizabeth A. Killion[1]*, Jinghong Wang[2]*, Junming Yie[1]*†, Stone D.-H. Shi[3], Darren Bates[3], Xiaoshan Min[4], Renee Komorowski[1], Todd Hager[5], Liying Deng[1], Larissa Atangan[1], Shu-Chen Lu[1], Robert J. M. Kurzeja[1], Glenn Sivits[1], Joanne Lin[3], Qing Chen[3], Zhulun Wang[4], Stephen A. Thibault[4], Christina M. Abbott[3], Tina Meng[3], Brandon Clavette[6], Christopher M. Murawsky[6], Ian N. Foltz[6], James B. Rottman[7], Clarence Hale[1], Murielle M. Véniant[1], David J. Lloyd[1]‡

Glucose-dependent insulinotropic polypeptide (GIP) receptor (GIPR) has been identified in multiple genome-wide association studies (GWAS) as a contributor to obesity, and GIPR knockout mice are protected against diet-induced obesity (DIO). On the basis of this genetic evidence, we developed anti-GIPR antagonistic antibodies as a potential therapeutic strategy for the treatment of obesity and observed that a mouse anti-murine GIPR antibody (muGIPR-Ab) protected against body weight gain, improved multiple metabolic parameters, and was associated with reduced food intake and resting respiratory exchange ratio (RER) in DIO mice. We replicated these results in obese nonhuman primates (NHPs) using an anti-human GIPR antibody (hGIPR-Ab) and found that weight loss was more pronounced than in mice. In addition, we observed enhanced weight loss in DIO mice and NHPs when anti-GIPR antibodies were codosed with glucagon-like peptide-1 receptor (GLP-1R) agonists. Mechanistic and crystallographic studies demonstrated that hGIPR-Ab displaced GIP and bound to GIPR using the same conserved hydrophobic residues as GIP. Further, using a conditional knockout mouse model, we excluded the role of GIPR in pancreatic β-cells in the regulation of body weight and response to GIPR antagonism. In conclusion, these data provide preclinical validation of a therapeutic approach to treat obesity with anti-GIPR antibodies.

INTRODUCTION

Glucose-dependent insulinotropic polypeptide (GIP) and glucagon-like peptide-1 (GLP-1) are gut-derived incretin hormones, known for their ability to augment glucose-stimulated insulin secretion and, in the case of GLP-1, also to promote satiety. GLP-1 analogs are marketed for the treatment of type 2 diabetes (T2D) and obesity. GIP agonists, on the other hand, have not been developed for these diseases, owing to its impaired insulinotropic effect in patients with T2D (*1*).

GIP is secreted from K cells located in the proximal small intestine, whereas GLP-1 is secreted from L cells located in the lower small intestine and colon. Dietary carbohydrate and fat are potent stimulants of GIP secretion in humans (*2*), and meal size (*3*) and obesity (*4*), but not diabetes (*5*), are positively correlated with postprandial GIP secretion (*3*). High-fat diet (HFD)–fed rodents have increased GIP secretion from K cells (*6*, *7*), and similarly, acute HFD feeding in humans also results in 42% increase in circulating GIP concentrations before any noticeable body weight increase (*8*), indicating a positive correlation between exposure to HFD and GIP concentrations. As a result, HFD and elevated systemic concentrations of GIP may underlie differences in adiposity between human subjects.

GIP activity in the pancreas and potentiation of insulin secretion are elicited via G_s protein signaling and cyclic adenosine monophosphate (cAMP) production by activation of the GIP receptor (GIPR). The incretin effect of GIP is ablated in GIPR knockout (KO) mice that exhibit impaired oral glucose tolerance as a result of reduced insulin secretion (*9*). GIP also directly activates GIPR in adipocytes (*10*), resulting in fatty acid uptake and incorporation into adipose tissues (*11*), possibly via lipoprotein lipase (*12*); promotes glucose uptake, fatty acid synthesis, and fatty acid incorporation into triglycerides; and stimulates lipolysis and subsequent fatty acid reesterification (*13*–*16*).

GIPR has been identified in genome-wide association studies (GWAS) of body mass index (BMI) measurements (*17*), and the single-nucleotide polymorphism (SNP) *rs1800437* in *GIPR* results in a nonsynonymous change, altering the protein sequence from glutamic acid to glutamine at residue 354 (E354Q), and the associated obesity risk allele E354, leading to an obesity odds ratio of 1.1 (*17*). Reciprocally, Q354 is associated with a reduced incretin effect (*18*) and delayed GIPR membrane recycling (*19*), suggesting that Q354 exhibits lower GIPR activity than E354, allowing speculation that higher GIPR activity is obesity promoting. This is validated by the observations that GIP, K cell, and GIPR KO mice are all resistant to HFD-induced obesity and insulin resistance (*9*, *20*, *21*).

Together, the mouse and human genetic evidence, coupled with the established role of GIPR in pancreatic β-cells and adipocytes, supports the concept of developing a therapeutic GIPR antagonist for the treatment of obesity. For these reasons, we developed both mouse anti-murine (muGIPR-Ab) and human anti-human antagonistic antibodies (hGIPR-Ab) against GIPR and evaluated their pharmacological activity in vitro and in obese mice and NHPs.

[1]Amgen Research, Department of Cardiometabolic Disorders, Amgen Inc., One Amgen Center Dr., Thousand Oaks, CA 91320, USA. [2]Amgen Research, Department of Cardiometabolic Disorders, Amgen Inc., 1120 Veterans Blvd., South San Francisco, CA 94080, USA. [3]Amgen Research, Department of Therapeutic Discovery, Amgen Inc., One Amgen Center Dr., Thousand Oaks, CA 91320, USA. [4]Amgen Research, Department of Therapeutic Discovery, Amgen Inc., 1120 Veterans Blvd., South San Francisco, CA 94080, USA. [5]Amgen Research, Department of Pharmacokinetics and Drug Metabolism, Amgen Inc., One Amgen Center Dr., Thousand Oaks, CA 91320, USA. [6]Amgen Research, Department of Therapeutic Discovery, Amgen Inc., 7990 Enterprise Street, Burnaby, BC V5A 1V7, Canada. [7]Amgen Research, Comparative Biology and Safety Sciences, Amgen Inc., 360 Binney St., Cambridge, MA 02141, USA.
*These authors contributed equally to this work.
†Present address: Merck Research Laboratories, 2015 Galloping Hill Rd., Kenilworth, NJ 07033, USA.
‡Corresponding author. Email: dlloyd@amgen.com

RESULTS

A mouse anti-murine GIPR antibody prevents body weight gain in diet-induced obese mice

We developed a mouse anti-murine monoclonal GIPR antibody (muGIPR-Ab) that fully neutralized GIPR activity by inhibiting cAMP production in mouse GIPR–expressing cells in vitro (Fig. 1A). To evaluate muGIPR-Ab in vivo, we developed a pharmacodynamic (PD) assay based on the insulinotropic effect of GIP. Using a long-acting GIP analog, [D-Ala^2]-GIP (DA-GIP), we carried out a modified glucose tolerance test (GTT) in diet-induced obesity (DIO) mice. Glucose and DA-GIP challenge increased serum insulin concentrations at 30 min and reduced blood glucose excursion at 60 min compared to glucose and vehicle only (Fig. 1, B and C, black and white bars, respectively). Treatment of DIO mice with muGIPR-Ab before the PD assay dose-dependently abolished the insulinotropic effect of DA-GIP (Fig. 1B) and resulted in higher glucose concentrations at 60 min (Fig. 1C), demonstrating that muGIPR-Ab was also an effective GIPR antagonist in vivo. Serum concentrations of muGIPR-Ab were measured to establish a pharmacokinetic (PK)–PD relationship and in vivo half-maximal inhibitory concentration (IC_{50}) of 42.4 nM and half-maximal response (EC_{50}) of 122 nM with insulin and glucose concentrations, respectively (fig. S1, A and B).

To determine the chronic effect of muGIPR-Ab in DIO mice, we dosed muGIPR-Ab or a non-neutralizing anti-GIPR antibody (CTL-Ab) for 45 days. muGIPR-Ab treatment resulted in lower body weights than the CTL-Ab treatment (Fig. 1, D and E). After 33 days of treatment, fat mass was, on average, 37% lower (Fig. 1F), with a minimal (5.3%) change in lean mass (Fig. 1G) in mice treated with muGIPR-Ab (30 mg/kg) compared to CTL-Ab. These findings were supported by reduced white adipose tissue (WAT) mass (Fig. 1H), and this reduction in adiposity was reinforced by reduced macrophage infiltration we observed in epididymal WAT as indicated by F4/80 immunostaining (fig. S2A).

Fasting blood glucose and serum insulin concentrations were reduced in mice treated with muGIPR-Ab compared to CTL-Ab (Fig. 1, I and J), whereas there was no improvement in glucose tolerance in an intraperitoneal GTT (IPGTT), which directly assessed glucose tolerance without being confounded by the possible alteration of incretin function (Fig. 1K). Further, treatment with muGIPR-Ab reduced liver weight and triglyceride concentrations compared to CTL-Ab (fig. S2, B and C). These improvements were supported by reduced lipid-rich cytoplasmic microvesicles in midzonal/centrilobular hepatocytes, as assessed by analyzing hematoxylin and eosin– and adipophilin-stained sections (fig. S2D).

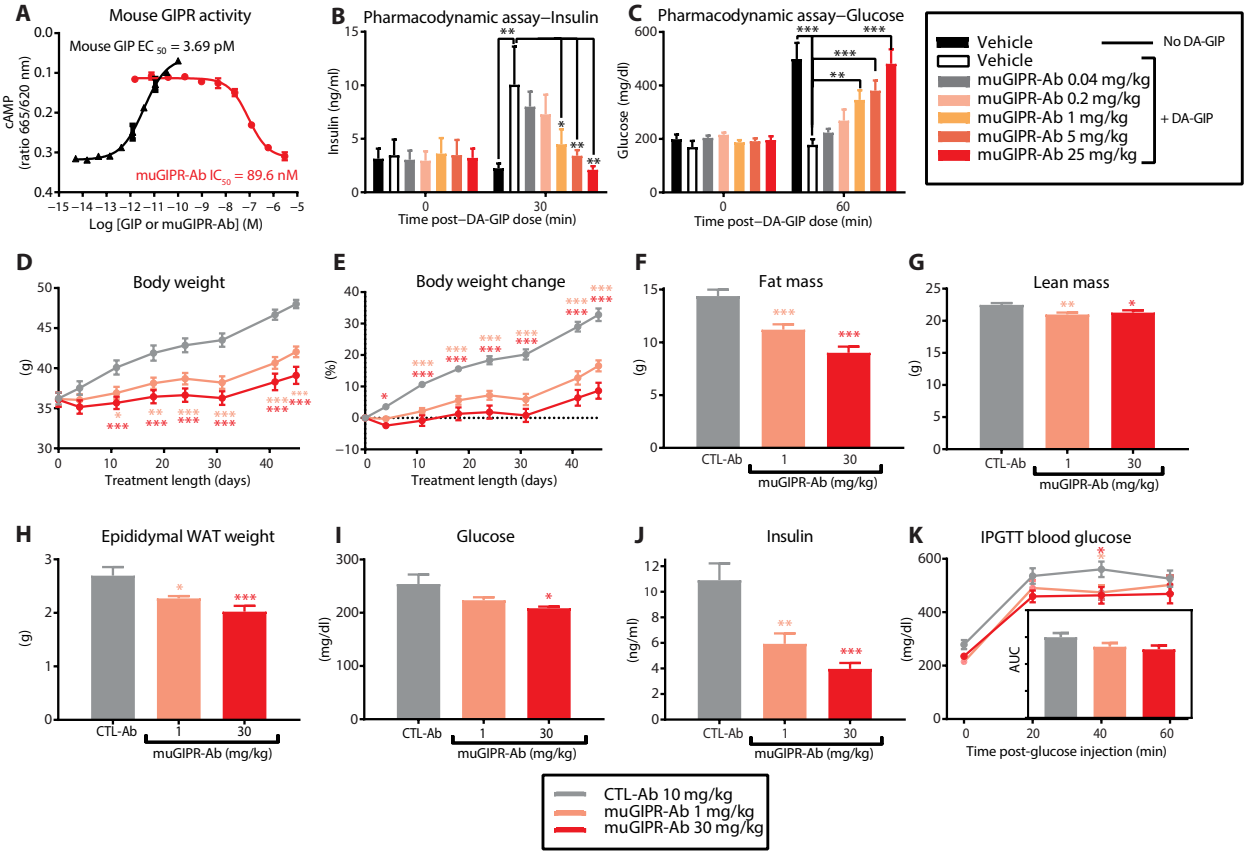

Fig. 1. muGIPR-Ab prevents weight gain in DIO mice. (**A**) cAMP in cells expressing mouse GIPR with mouse GIP (black) or muGIPR-Ab + 15 pM mouse GIP (red) ($n = 2$ replicates per treatment). (**B**) Serum insulin and (**C**) blood glucose concentrations were measured after intraperitoneal injection of DA-GIP (50 nmol/kg) and glucose (2 g/kg) in DIO mice pretreated with vehicle or muGIPR-Ab ($n = 8$ mice per group). (**D** to **K**) DIO mice fed HFD for 11 weeks were treated with control antibody (CTL-Ab) or muGIPR-Ab ($n = 10$ mice per group). (D) Body weight was measured and used to calculate (E) percent change in body weight from day 0 to 46. (F) Fat mass and (G) lean mass were determined on day 33. (H) Epididymal WAT weight was measured at the end of the study. Four-hour fasting (I) blood glucose and (J) serum insulin concentrations were measured on day 35. (K) IPGTT was conducted on day 28, and post-challenge blood glucose area under the curve (AUC) was calculated (inset). Data represent means ± SEM. One- or two-way repeated-measures analysis of variance (ANOVA) with Sidak's test for multiple comparisons [F to K (inset) and B, C, and K, respectively]; $^*P < 0.05$, $^{**}P < 0.01$, and $^{***}P < 0.001$ versus control (vehicle either with or without DA-GIP) as indicated (B and C) or versus CTL-Ab (D to K).

muGIPR-Ab enhances body weight loss in combination with the GLP-1R agonist liraglutide in DIO mice

Next, we compared muGIPR-Ab to a current anti-obesity standard of care, the GLP-1 analog liraglutide. DIO mice were administered vehicle, muGIPR-Ab alone, liraglutide alone, or a combination of muGIPR-Ab and liraglutide for 38 days. By the end of the study, the vehicle group increased in body weight by 5.4%, muGIPR-Ab alone prevented body weight gain (because this group only gained 0.5% from baseline), and liraglutide alone resulted in 7.2% weight loss (Fig. 2, A and B). The combination of muGIPR-Ab and liraglutide resulted in 23.5% weight loss (Fig. 2, A and B), which is greater than the potential additive effect of the two therapies alone. Fat (Fig. 2C) and lean mass (fig. S3A) were reduced in both the liraglutide alone and combination groups compared to vehicle, and changes in fat mass were also reflected in WAT weights (fig. S3, B and C). Liver weight also decreased in all groups receiving treatment (fig. S3D). Food consumption was measured during treatment days 1 to 4 and days 21 to 24 and was unchanged by muGIPR-Ab alone (Fig. 2D). Both liraglutide alone and the combination treatment resulted in greater than 50% reduction in food intake during days 1 to 4 (Fig. 2D), an effect that waned by the end of the study (Fig. 2D, days 21 to 24). Despite the enhanced weight loss by the combination of muGIPR-Ab and liraglutide, the anorectic effects were not similarly decreased when the two molecules were combined (Fig. 2D). Consistent with the data presented in Fig. 1 (I and J), muGIPR-Ab reduced fasting blood glucose and serum insulin concentrations compared to vehicle, and as expected, liraglutide improved both measures (Fig. 2, E and F). muGIPR-Ab and liraglutide combined resulted in reduced insulin concentrations compared to liraglutide alone (Fig. 2F). In this study, we chose to directly assess glucose tolerance in the context of any potential incretin changes by challenging the animals with an oral GTT (OGTT). Glucose tolerance was unchanged with muGIPR-Ab treatment compared to vehicle but was similarly improved by liraglutide alone and the combination treatment (Fig. 2, G and H).

To find any hormonal changes that might underpin the anti-obesity effects of muGIPR-Ab, we analyzed terminal serum samples for pancreatic- and digestive-related hormones (fig. S3E). We found that peptide YY, pancreatic polypeptide, ghrelin, glucagon, and amylin were not altered by muGIPR-Ab treatment alone or in combination with liraglutide (fig. S3E). GIP concentrations were not altered by muGIPR-Ab but were reduced in the liraglutide alone and combination groups (fig. S3E). GLP-1 concentrations were increased only by liraglutide alone, possibly a result of assay cross-reactivity with liraglutide (fig. S3E). Consistent with the observed insulin changes, C-peptide concentrations were reduced in all treatment groups (fig. S3E).

Despite improvements in fasting blood glucose and serum insulin concentrations and reductions in adiposity in the muGIPR-Ab–treated DIO mice, glucose tolerance was not improved (Figs. 1K and 2G). This discrepancy in glucose homeostasis could reflect an alteration in incretin function due to reduced GIPR β-cell activity. To explore this more carefully, we conducted an OGTT in DIO mice after a single muGIPR-Ab injection and assessed insulin secretion 24 hours after treatment (fig. S4, A and B). Glucose tolerance was unchanged by muGIPR-Ab despite diminished insulin secretion, demonstrating that although incretin function was altered, glucose tolerance remained intact, possibly reflecting peripheral improvements in glucose homeostasis with muGIPR-Ab. These data demonstrate that although glucose tolerance was not improved as measured by blood glucose concentrations per se, glucose homeostasis was improved when considering the accompanying reductions in insulin concentrations, in both the fasting (Figs. 1J and 2F) and postprandial states (fig. S4B).

Up to this point, we had administered muGIPR-Ab twice weekly at doses of ≥25 mg/kg to ensure maximal target coverage and weight loss effects. We next determined the PK of muGIPR-Ab to allow a more precise dosing regimen. After a single intraperitoneal injection, muGIPR-Ab demonstrated a terminal half-life ($t_{1/2,z}$) of 11.9 to 13.4 days and an apparent clearance (CL/F) of 2.2 to 2.5 ml day^{-1} kg^{-1} over a dose

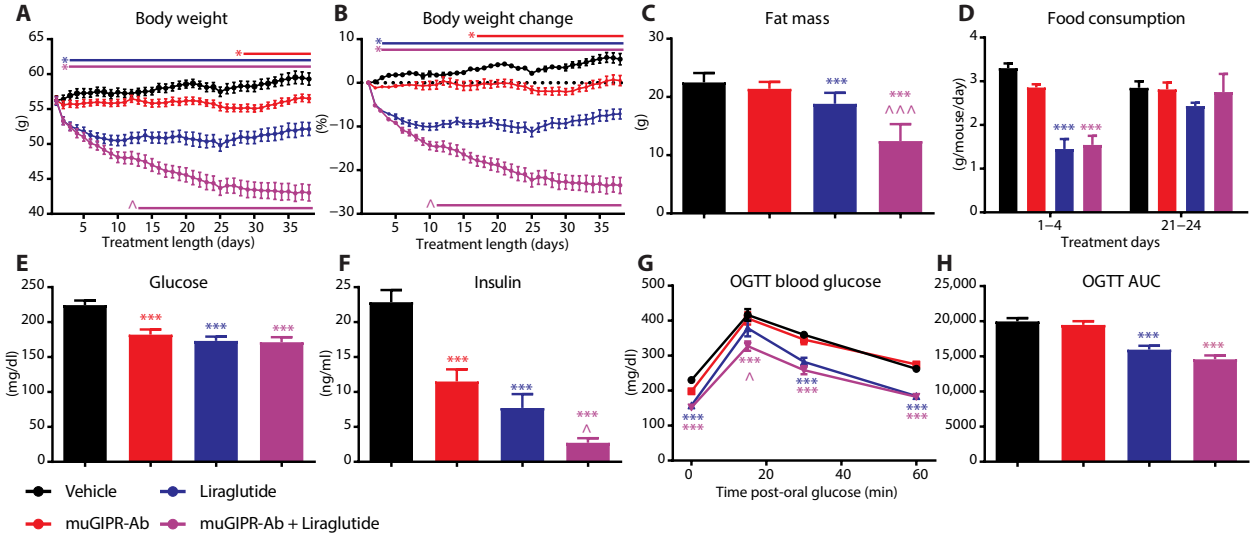

Fig. 2. muGIPR-Ab enhances body weight loss in combination with the GLP-1R agonist liraglutide in DIO mice. Established DIO mice fed HFD for 30 weeks were treated with vehicle, muGIPR-Ab (30 mg/kg, twice a week), and liraglutide (0.3 mg/kg, once a day) alone or in combination ($n = 10$ mice per group unless otherwise specified). (**A**) Body weight was measured and used to calculate (**B**) percent change. (**C**) Fat mass was measured on day 38. (**D**) Food consumption was measured during treatment days 1 to 4 and 22 to 24 ($n = 3$ to 8 mice per group). (**E**) Fasting blood glucose and (**F**) serum insulin concentrations were measured on day 39. (**G**) OGTT was performed on day 25 from which (**H**) AUC was calculated. Data represent means ± SEM. One- or two-way repeated-measures ANOVA both with Sidak's test for multiple comparisons (C, E, F, and H and A, B, D, and G, respectively); *$P < 0.05$ and ***$P < 0.001$ versus vehicle; ^$P < 0.05$ and ^^^$P < 0.001$, liraglutide versus muGIPR-Ab + liraglutide.

range of 1 to 100 mg/kg (fig. S5). A maximum effect in the acute PD assay was achieved with muGIPR-Ab (25 mg/kg), which correlated with a mean serum concentration of 2250 nM (fig. S1, A and B), and allowed us to determine that muGIPR-Ab (25 to 30 mg/kg) dosed weekly was sufficient to provide maximal target coverage, and we adjusted subsequent experimental dosing accordingly.

The enhanced weight loss of the muGIPR-Ab and liraglutide combination also extended to the other GLP-1R agonists exendin-4 and dulaglutide (Fig. 3, A and B). Heavier DIO mice were treated with muGIPR-Ab, each GLP-1R agonist, or a combination of muGIPR-Ab and each agonist (Fig. 3, A and B), and in each case, the combination treatment resulted in a greater body weight reduction than the monotherapy.

To investigate whether muGIPR-Ab could augment weight loss preestablished by liraglutide, we sequentially dosed muGIPR-Ab after a period of liraglutide treatment. DIO mice were administered two doses of liraglutide for 2 weeks to establish stable weight loss and were then further subdivided into two groups: one to receive liraglutide treatment only and the other to additionally receive muGIPR-Ab for 2 weeks. In both liraglutide dose groups, muGIPR-Ab enhanced the preestablished weight loss (Fig. 3, C and D), demonstrating that simultaneous combination therapy is not essential for the enhanced effect of the GLP-1R agonists and GIPR antagonism on weight loss. At the initiation of the muGIPR-Ab augmentation period, we observed a reduction in food intake in each combination group compared to the control group maintained on liraglutide only (Fig. 3E, days 15 to 17). This additional anorectic effect of sequential combination was not observed with simultaneous combination (Fig. 3E), suggesting that our ability to detect an effect on food intake was improved with this sequential study design.

To further explore the effect on food consumption, we assessed the potential of muGIPR-Ab to sensitize DIO mice to the anorectic effects of GLP-1R agonism. DIO mice were pretreated with muGIPR-Ab for 24 hours and then treated with a dose range of liraglutide, and body weight and food consumption were measured after 24 hours. A small improvement in weight loss by muGIPR-Ab and liraglutide was observed compared to liraglutide alone at the highest dose (Fig. 3F), consistent with the observations of chronic weight loss; however, muGIPR-Ab did not increase in vivo anorectic sensitivity to liraglutide on food intake (Fig. 3G).

The ability of muGIPR-Ab to prevent weight gain alone and to reduce body weight in combination with GLP-1R agonism is independent of pancreatic β-cell GIPR

On the basis of findings by Campbell *et al.* (*22*) showing that mice with β-cell–specific KO of GIPR have increased sensitivity to exogenous GLP-1–stimulated insulin secretion, we hypothesized that inhibition of GIPR in pancreatic β-cells by muGIPR-Ab may also sensitize mice to GLP-1–mediated weight loss. Therefore, we generated GIPR-floxed mice ($Gipr^{fl/fl}$) (schematic representation in fig. S6A), and the $Gipr^{fl/fl}$ mouse was mated to a mouse expressing *Cre* recombinase driven by the rat insulin promoter, which we subsequently confirmed by test mating to R26R mice (fig. S6B) (*23*) to produce a line of GIPR β-cell–specific KO mice ($Gipr^{-/-\beta Cell}$). *Gipr* RNA expression was reduced by 65% in isolated pancreatic islets from $Gipr^{-/-\beta Cell}$ mice compared to $Gipr^{fl/fl}$ littermates, with residual *Gipr* expression in islets likely from non–β-cells in the islets (Fig. 4A) (*24*, *25*). We confirmed that GIPR activity was ablated in β-cells by demonstrating that $Gipr^{-/-\beta Cell}$ mice were refractory to GIP-stimulated insulin secretion (Fig. 4B).

Consistent with the previously published model (*22*), $Gipr^{-/-\beta Cell}$ mice showed no differences in body weight (Fig. 4C) or fat mass (Fig. 4D) compared to $Gipr^{fl/fl}$ mice after 11 weeks of HFD feeding. However, $Gipr^{-/-\beta Cell}$ mice had a 2-g reduction in lean mass compared to $Gipr^{fl/fl}$ (fig. S6C), which had not been previously reported. In addition, $Gipr^{-/-\beta Cell}$ mice demonstrated 30% lower fasting blood glucose (Fig. 4E) without a difference in fasting serum insulin (Fig. 4F), which suggests improved insulin sensitivity compared to $Gipr^{fl/fl}$ mice in line with the improved homeostatic model of insulin resistance (HOMA-IR) (Fig. 4G).

To determine the role of β-cell GIPR in the prevention of body weight gain by muGIPR-Ab or in weight loss when combined with GLP-1R agonism, we treated the same $Gipr^{fl/fl}$ and $Gipr^{-/-\beta Cell}$ mice previously fed a HFD for 11 weeks with vehicle, muGIPR-Ab alone, dulaglutide alone, or a combination of muGIPR-Ab and dulaglutide for 38 days. In this case, we chose dulaglutide because we had demonstrated that the enhanced effects of muGIPR-Ab with liraglutide were also observed with dulaglutide (Fig. 3, A and B). $Gipr^{fl/fl}$ and $Gipr^{-/-\beta Cell}$ mice did not differ in their body weight response to any of the treatments (Fig. 4, H and I, and fig. S6, D and E). Furthermore, $Gipr^{fl/fl}$ and $Gipr^{-/-\beta Cell}$ mice did not differ in fat mass, lean mass, inguinal WAT weight, or liver weight in response to any treatment (Fig. 4J and fig. S6, F to H, respectively); however, a small reduction was observed in the epididymal WAT weights of $Gipr^{-/-\beta Cell}$ mice treated with muGIPR-Ab compared to $Gipr^{fl/fl}$ mice treated with muGIPR-Ab (fig. S6I). In addition, no differences were detected in food consumption between the two lines of mice within each treatment group (fig. S6J).

Glucose homeostasis was similarly improved by both the dulaglutide alone and the combination treatment in both lines of mice, as illustrated by lower blood glucose (Fig. 4K) and serum insulin concentrations (Fig. 4L). Vehicle-treated $Gipr^{-/-\beta Cell}$ mice had lower HOMA-IR compared to vehicle-treated $Gipr^{fl/fl}$ mice, and $Gipr^{fl/fl}$ mice treated with muGIPR-Ab similarly improved HOMA-IR (Fig. 4M), indicating a possible role for β-cell GIPR in the regulation of glucose homeostasis independent of weight loss.

Because these data establish a lack of an effect of GIPR in β-cells for the mechanism of muGIPR-Ab to prevent weight gain, we investigated differences in adipose-specific hormones in terminal serum samples. We observed no differences between treatment groups or between lines of mice, other than the expected decrease in leptin associated with decreased fat mass after combination treatment (fig. S6K).

muGIPR-Ab reduces food consumption and the respiratory exchange ratio in DIO mice

To identify any physiological changes that could account for the anti-obesity effects of muGIPR-Ab, we performed indirect calorimetry continuously in DIO mice treated with either vehicle, muGIPR-Ab, or CTL-Ab for 40 days. To mimic the study in Fig. 1D, we chose DIO mice with a short pre-exposure to HFD to maximize the potential effects of muGIPR-Ab. As expected, muGIPR-Ab prevented weight gain (Fig. 5, A and B) and was associated with reduced cumulative food consumption (Fig. 5C). No changes were observed in oxygen consumption (VO_2) or in carbon dioxide production (VCO_2) (Fig. 5, D and E, respectively). There was a pronounced reduction in the respiratory exchange ratio (RER) during the light period of muGIPR-Ab–treated mice, reflecting greater lipid oxidation in resting mice (Fig. 5F). Physical activity was unchanged by muGIPR-Ab treatment (Fig. 5G).

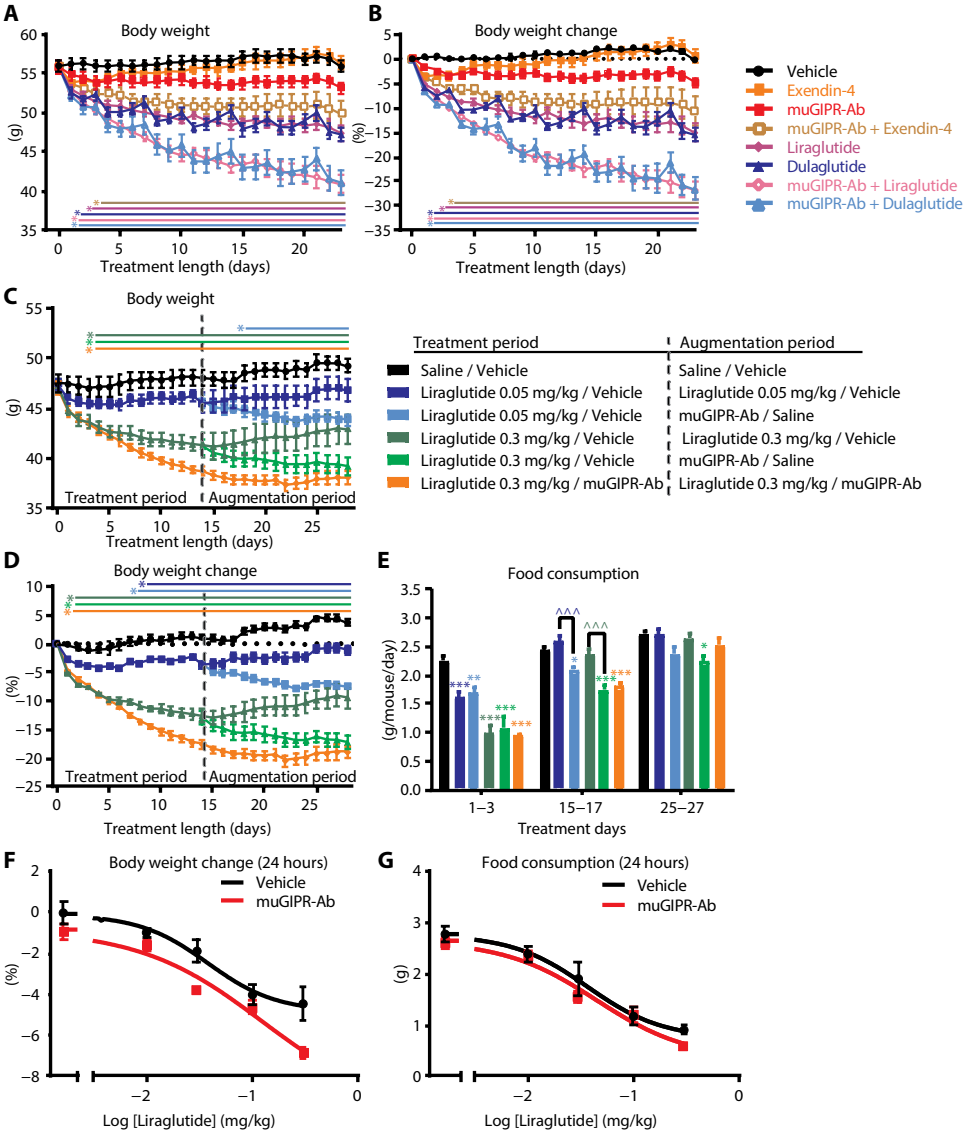

Fig. 3. muGIPR-Ab results in weight loss in DIO mice in combination with various GLP-1R agonists without sensitizing mice to anorectic effects of a GLP-1R agonist. (**A** and **B**) Established DIO mice fed HFD for 31 weeks were treated with multiple GLP-1 analogs alone or in combination with muGIPR-Ab for 23 days with vehicle, muGIPR-Ab (25 mg/kg, once a week), dulaglutide (1 mg/kg, twice a week), liraglutide (0.3 mg/kg, once a day), exendin-4 (0.01 mg/kg, once a day), or combinations using the same dose frequency. (A) Body weight was measured and used to calculate (B) percent change in body weight from day 0 to 23 ($n = 8$ mice per group). (**C** to **E**) Established DIO mice fed HFD for 13 weeks were initially treated during the "treatment period" with vehicle, liraglutide (0.05 or 0.3 mg/kg, once a day), or liraglutide (0.3 mg/kg, once a day) in combination with muGIPR-Ab (25 mg/kg, once a week) for 14 days. On day 15, liraglutide-dosed mice were divided into two groups and either maintained on liraglutide or treated in combination with muGIPR-Ab (25 mg/kg, once a week) during the "augmentation period" ($n = 8$ mice per group unless otherwise specified). (C) Body weight was measured over time and used to (D) calculate percent change in body weight from day 0 to 28. (E) Food consumption per day measured during treatment days 1 to 3, 15 to 17, and 25 to 27. Data represent means ± SEM. (A to D) Two-way repeated-measures ANOVA with Sidak's test for multiple comparisons; (E) one-way ANOVA with Sidak's test for multiple comparisons at each time point. $^{*}P < 0.05$, $^{**}P < 0.01$, and $^{***}P < 0.001$ versus saline + vehicle; $^{\wedge\wedge\wedge}P < 0.001$, liraglutide versus muGIPR-Ab + liraglutide at the same liraglutide dose. (**F** and **G**) Established DIO mice fed HFD for 15 weeks were pretreated (for 24 hours) with either vehicle or muGIPR-Ab (10 mg/kg) and then treated with liraglutide or saline. (F) Body weight change and (G) food consumption were measured after 24 hours. Each data point represents means ± SEM of $n = 6$ mice per group.

Fully human anti-GIPR antibody specifically inhibits GIPR activity in vitro and in human adipocytes and islets ex vivo by displacing GIP

We identified a fully human monoclonal anti-human GIPR antibody (hGIPR-Ab) to further pursue GIPR antagonism as a potential therapeutic strategy for obesity. hGIPR-Ab antagonized human GIPR activity by inhibiting GIP-induced cAMP production in cells expressing human GIPR or nonhuman primate (NHP) GIPR (IC_{50} = 23.8 nM and IC_{50} = 15.1 nM, respectively) (Fig. 6, A and B). hGIPR-Ab was specific to GIPR and did not antagonize the glucagon receptor (GCGR) or GLP-1R (Fig. 6C). Binding of hGIPR-Ab to human GIPR membranes was measured using KinExA technology, and the equilibrium dissociation constant (K_D) was determined as 61 pM (Fig. 6D). To further explore the mechanism of GIPR antagonism, we investigated the displacement of ^{125}I-GIP by hGIPR-Ab from binding to membranes expressing human GIPR and demonstrated that hGIPR-Ab prevents GIP binding (hGIPR-Ab IC_{50} = 0.239 nM and GIP IC_{50} = 0.415 nM; Fig. 6E). To confirm whether GIPR antagonism of hGIPR-Ab occurred via GIP displacement, we solved the structure of the human GIPR extracellular domain (ECD) complex with the antigen-binding fragment (Fab) of hGIPR-Ab at 1.9 Å resolution [Protein Data Bank (PDB) code: 6DKJ] (Fig. 6F). Human GIPR ECD adopts an α-β-β-α fold that is common to other class B G protein–coupled receptor (GPCR) ECDs, including GCGR and GLP-1R (*26*–*28*). The C-terminal stalk between the core ECD and the transmembrane domain (amino acids 123 to 134), which is disordered in previously solved structures, adopted a two-turn helix and was packed against the antibody framework. The buried solvent-accessible surface area on human GIPR was 1184 Å^2, of which 917 Å^2 was contributed by the hGIPR-Ab heavy chain and 267 Å^2 by the light chain. The complementarity score was 0.616, which is typical of antibody-antigen interactions. To understand the effect of antibody on the ligand binding, we superposed our structure of human GIPR ECD–hGIPR-Ab Fab onto the reported structure of the GIPR-GIP complex (PDB code: 2QKH) (*27*). hGIPR-Ab completely occluded the C terminus of the GIP peptide, thus preventing the binding of GIP to the GIPR ECD (Fig. 6F). Four hydrophobic residues in hGIPR-Ab, including Trp^{52} and Phe^{53} from complementarity-determining

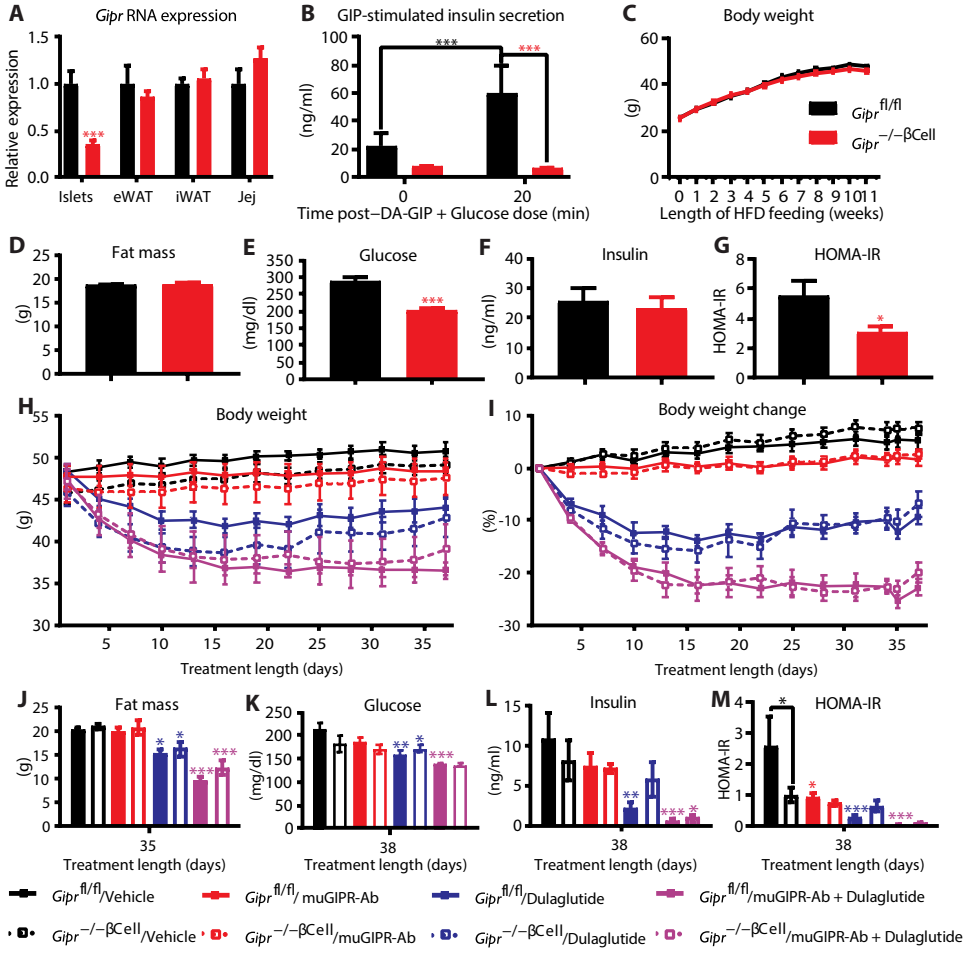

Fig. 4. The effect of muGIPR-Ab to prevent weight gain alone and to reduce body weight in combination with GLP-1R agonism is independent of pancreatic β-cell GIPR. (**A**) *Gipr* RNA expression in isolated pancreatic islets and *Gipr*-expressing tissues [epididymal WAT (eWAT), inguinal WAT (iWAT), and jejunum (Jej)] in $Gipr^{fl/fl}$ and $Gipr^{-/-\beta Cell}$ mice fed HFD for 15 weeks ($n = 5$ to 8 mice per group). (**B**) Serum insulin was measured before and after intraperitoneal injection of DA-GIP (50 nmol/kg) and glucose (1 g/kg) in $Gipr^{fl/fl}$ and $Gipr^{-/-\beta Cell}$ male mice fed HFD for 11 weeks ($n = 6$ to 8 mice per group). (**C** to **G**) $Gipr^{fl/fl}$ and $Gipr^{-/-\beta Cell}$ male mice fed HFD for 11 weeks ($n = 27$ to 30 mice per group). (C) Body weight was measured during HFD feeding. (D) Fat mass, (E) fasting blood glucose, and (F) serum insulin values were measured and used to calculate a (G) HOMA-IR. (**H** to **M**) $Gipr^{fl/fl}$ and $Gipr^{-/-\beta Cell}$ male mice fed HFD for 11 weeks treated for 38 days with vehicle, muGIPR-Ab (25 mg/kg every 6 days), dulaglutide (1 mg/kg every 3 days), or combination ($n = 6$ to 8 mice per group). (H) Body weight was measured and used to calculate (I) percent change in body weight from day 1 to 38. (J) Fat mass was measured on day 35 of treatment. (K) Fasting blood glucose and (L) serum insulin values were measured and used to calculate (M) HOMA-IR on day 38. Data represent means ± SEM and were statistically assessed using (A and D to G) one-way ANOVA $Gipr^{fl/fl}$ versus $Gipr^{-/-\beta Cell}$, (C) repeated-measures two-way ANOVA $Gipr^{fl/fl}$ versus $Gipr^{-/-\beta Cell}$, (H and I) no statistics shown for simplicity, and (J to G) one-way ANOVA with Sidak's test for multiple comparisons. $^{*}P < 0.05$, $^{**}P < 0.01$, and $^{***}P < 0.001$, $Gipr^{fl/fl}$ vehicle versus $Gipr^{fl/fl}$ treated, $Gipr^{-/-\beta Cell}$ vehicle versus $Gipr^{-/-\beta Cell}$ treated, or $Gipr^{fl/fl}$ versus $Gipr^{-/-\beta Cell}$ within each treatment (indicated with a bracket).

region (CDR) H2 and Ile[102] and Phe[103] from CDRH3, were perfectly aligned with the four conserved hydrophobic residues from GIP: Phe[22], Val[23], Leu[26], and Leu[27] (fig. S7A). Comparing the epitope of hGIPR-Ab to that of GIP, there was almost complete overlap of the peptide binding groove, and hGIPR-Ab showed more extensive binding surface on the GIPR ECD (fig. S7, B and C).

Last, we sought to establish the effect of hGIPR-Ab in primary human cells known to express GIPR (*29*). We first determined GIP activity by measuring insulin secretion in primary human pancreatic microtissues (EC_{50} = 2.39 nM) and assessing cAMP production in primary human subcutaneous adipocytes (EC_{50} = 1.28 nM; Fig. 6, G and H), and subsequently established that hGIPR-Ab blocked GIPR activity in response to submaximal GIP stimulation (islets IC_{50} = 5.97 nM and adipocytes IC_{50} = 2.00 nM; Fig. 6, I and J).

hGIPR-Ab provides body weight loss alone and in combination with GLP-1R agonist dulaglutide in naïve spontaneously obese NHPs

We next assessed translational efficacy in spontaneously obese male NHPs. Preliminary assessments in NHPs revealed intolerability to GLP-1R agonists; thus, we established a protocol to progressively increase the dose of dulaglutide to minimize instances of vomiting. Animals were chronically treated for 18 days with either vehicle or dulaglutide given in a dose escalation regimen (0.05, 0.1, and 0.25 mg/kg for 6 days each). After 18 days, each group was further split into groups treated with or without hGIPR-Ab (3 mg/kg) for an additional 30 days. After day 48, all animals were monitored for an additional 28-day washout period.

At the end of treatment, vehicle-treated NHPs gained, on average, 6.2% body weight compared to baseline, and body weight reduction was observed in all three treatment groups when compared to their own baseline and to vehicle (Fig. 7, A and B). The combination group treated with hGIPR-Ab and dulaglutide demonstrated a greater body weight reduction (−14.5%) when compared to either hGIPR-Ab (−1.86%) or dulaglutide (−8.57%) treatments alone (Fig. 7, A and B). Food intake was reduced in all treatment groups compared to vehicle, with the greatest reduction observed in the combination hGIPR-Ab plus dulaglutide group (Fig. 7, C and D). The reduction in food intake was similar between the hGIPR-Ab and dulaglutide groups (Fig. 7, C and D), although the reduction in body weight was 4.5-fold greater than seen with dulaglutide alone. Food intake rebounded in the dulaglutide-only group and the combination treatments in the washout phase, whereas it was maintained in the hGIPR-Ab group, likely owing to the extended PK of hGIPR-Ab [$t_{1/2,z}$ = 10.3 to 13.3 days and systemic clearance (CL) = 4.1 to 4.9 ml day^{-1} kg^{-1} over a dose range of 0.1 to 3 mg/kg; fig. S8].

To evaluate the impact of GIPR antagonism on glucose homeostasis, we evaluated serum glucose and insulin concentrations and glucose tolerance. Glucose and insulin concentrations were not different between groups (Fig. 7, E and F). NHPs also underwent an

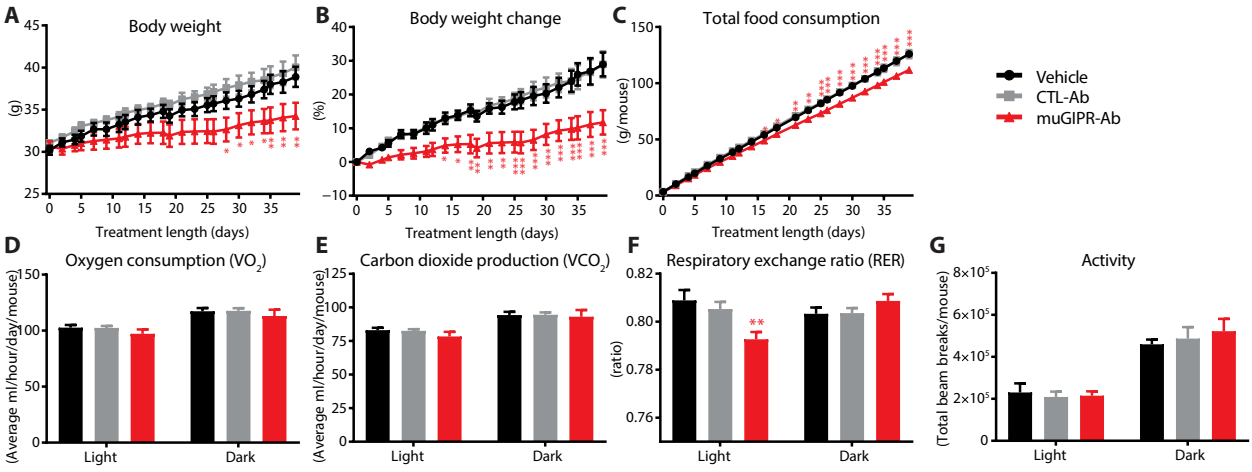

Fig. 5. muGIPR-Ab reduces food consumption and RER in DIO mice. Energy expenditure using indirect calorimetry was investigated continuously in DIO mice fed HFD for 7 weeks at the beginning of assessment treated with vehicle, CTL-Ab (30 mg/kg once per week), or muGIPR-Ab (30 mg/kg once per week) for 39 days ($n = 5$ to 6 mice per group). (**A**) Body weight was measured and used to calculate (**B**) percent change from day 1 to 39. (**C**) Cumulative food consumption was measured. (**D**) Average O_2 consumption (VO_2) and (**E**) CO_2 production (VCO_2) were measured over the entire experiment and used to calculate (**F**) RER. (**G**) Total physical activity measured for the entire experiment. Data represent means ± SEM. One- or two-way ANOVA both with Sidak's test for multiple comparisons (D to G and A to C, respectively); $^*P < 0.05$, $^{**}P < 0.01$, and $^{***}P < 0.001$ versus vehicle.

OGTT at the end of the treatment phase (Fig. 7G), and serum glucose and insulin concentrations during the OGTT were improved only in the dulaglutide and hGIPR-Ab combination group (Fig. 7, G and H); however, no changes were observed when expressed as AUC measures for any of the treatments (Fig. 7, I and J). GIPR antagonism did not worsen glucose tolerance. Only hGIPR-Ab treatment groups demonstrated reduced triglyceride concentrations compared to vehicle (Fig. 7K).

DISCUSSION

On the basis of human genetic associations, we set out to understand whether GIPR antagonism could be potentially used as a therapy to treat obesity. We found that treatment with muGIPR-Ab in DIO mice prevented body weight gain and hGIPR-Ab alone led to weight loss in obese NHPs, with a stronger impact on appetite than in mice. In addition, we found an enhanced effect on weight loss with the combination of GIPR antagonism and GLP-1R agonism in both obese mice and NHPs.

Recently, a neutralizing antibody (Gipg013) directed against GIPR (*30*) was identified and abolished the GIP-induced incretin effect in rat pancreatic islets. We demonstrated that hGIPR-Ab is also capable of blocking GIP activity in primary human adipocytes in addition to human pancreatic islets. Gipg013 was generated on a human immunoglobulin G (IgG) framework (*30*), suggesting possible therapeutic utility. However, to our knowledge, these GIPR antagonist therapies have not been further studied.

In contrast, neutralizing antibodies to GIP have been evaluated in mouse models of obesity and exhibited reduced weight gain in DIO mice (*31*). These previous data support our findings using both muGIPR-Ab and hGIPR-Ab, despite some differences, namely, that the GIP antibody does not fully prevent weight gain or alter food intake unlike the antibodies we present here. The differences in the observed weight loss effects in mice between our studies and the studies using GIP antibodies (*31*) could be due to slight differences in the study designs or innate difference in ligand versus receptor biology. Nonetheless, these data underpin the therapeutic potential of intervening in the GIP/GIPR axis for the treatment of obesity.

On the basis of GIPR's incretin effect, it would be expected that inhibiting pancreatic GIPR would lead to impaired glucose tolerance; however, in previous studies in mice with β-cell–specific KO of GIPR (*22*), and in our studies with $Gipr^{-/-\beta Cell}$ mice and with anti-GIPR antibodies in DIO mice and NHPs, no effect on glucose tolerance was observed. This is notable given the suppressed incretin response in mice treated with muGIPR-Ab and is possibly accounted for by improved peripheral glucose handling even after a single muGIPR-Ab treatment without changes in body weight; however, this has not been assessed in our current work.

Because islets from mice with GIPR β-cell–specific KO displayed enhanced glucose-stimulated insulin secretion in response to GLP-1 analog exendin-4 treatment (*22*), we theorized that the pancreatic β-cell GIPR activity may account for the weight loss effects by enhancing sensitivity to endogenous and/or exogenous GLP-1 analogs. However, we found that $Gipr^{-/-\beta Cell}$ mice were equally responsive to muGIPR alone, dulaglutide alone, and the combination compared to control $Gipr^{fl/fl}$ mice, suggesting that other GIPR-expressing tissues, such as the central nervous system (CNS) or adipose, are responsible for muGIPR-Ab's prevention of weight gain.

As antibodies are known not to penetrate the blood-brain barrier, we do not expect direct muGIPR-Ab or hGIPR-Ab antagonism in the CNS, unless GIPR can act directly or indirectly through the vagus nerve or area postrema. However, here, we reported the unexpected finding that muGIPR-Ab alone reduced food intake in DIO mice and to an even greater extent with hGIPR-Ab in obese NHPs. This finding has not been observed in GIPR KO mouse models (*9*, *22*, *32*) or in other therapies targeting the GIP/GIPR axis (*31*). Nonetheless, we hypothesized that GIPR antagonism could render the animal more sensitive to GLP-1. Here, we showed that, at least in an acute setting, liraglutide's anorectic effects were unchanged by muGIPR-Ab treatment in DIO mice, which excludes the possibility that muGIPR-Ab enhances exogenous GLP-1 anorectic sensitivity.

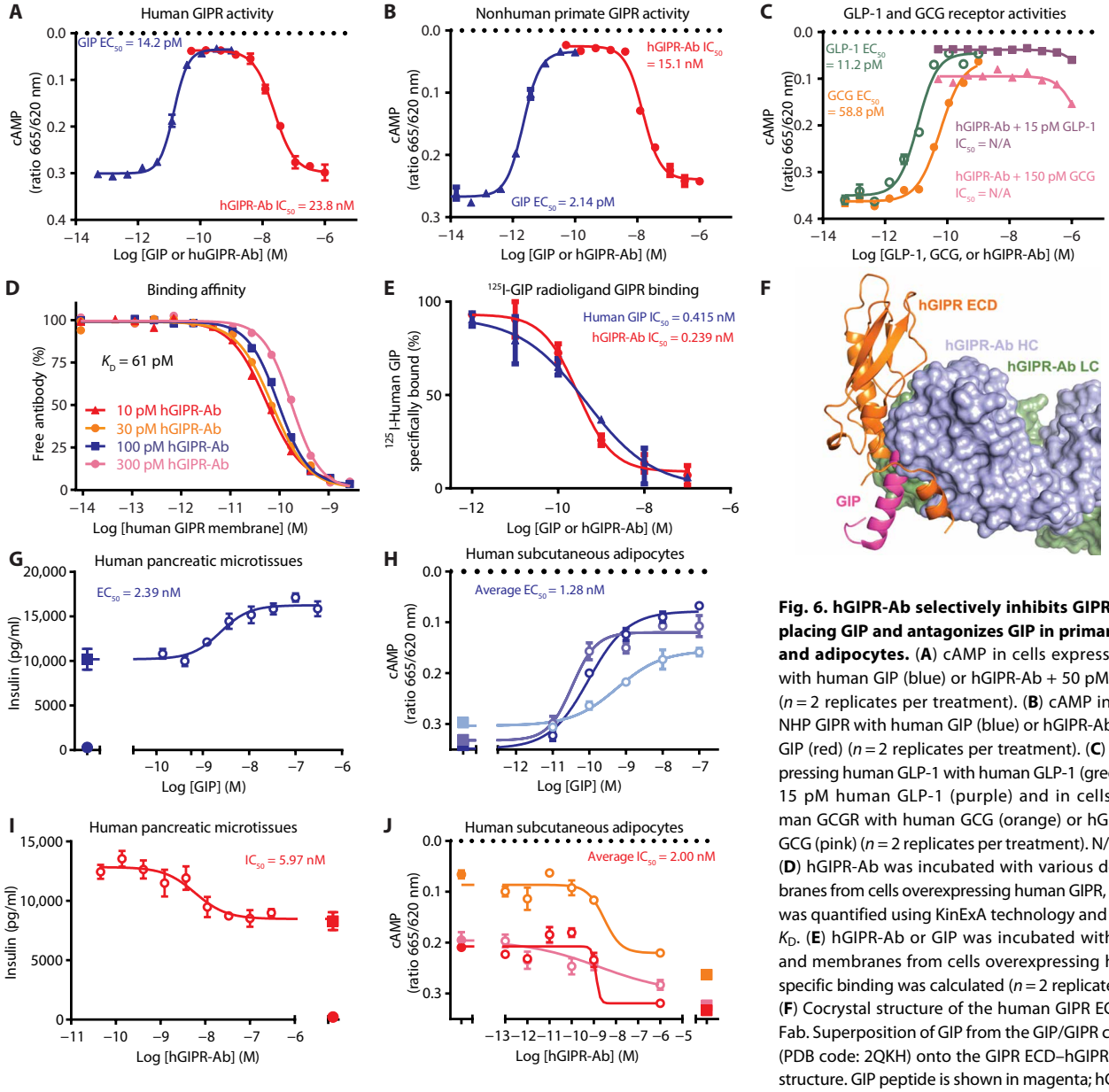

Fig. 6. hGIPR-Ab selectively inhibits GIPR activity by displacing GIP and antagonizes GIP in primary human β-cells and adipocytes. (**A**) cAMP in cells expressing human GIPR with human GIP (blue) or hGIPR-Ab + 50 pM human GIP (red) ($n = 2$ replicates per treatment). (**B**) cAMP in cells expressing NHP GIPR with human GIP (blue) or hGIPR-Ab + 50 pM human GIP (red) ($n = 2$ replicates per treatment). (**C**) cAMP in cells expressing human GLP-1 with human GLP-1 (green) or hGIPR-Ab + 15 pM human GLP-1 (purple) and in cells expressing human GCGR with human GCG (orange) or hGIPR-Ab + 150 pM GCG (pink) ($n = 2$ replicates per treatment). N/A, not applicable. (**D**) hGIPR-Ab was incubated with various densities of membranes from cells overexpressing human GIPR, and free antibody was quantified using KinExA technology and used to calculate K_D. (**E**) hGIPR-Ab or GIP was incubated with ^{125}I-human GIP and membranes from cells overexpressing human GIPR, and specific binding was calculated ($n = 2$ replicates per treatment). (**F**) Cocrystal structure of the human GIPR ECD and hGIPR-Ab Fab. Superposition of GIP from the GIP/GIPR complex structure (PDB code: 2QKH) onto the GIPR ECD–hGIPR-Ab Fab complex structure. GIP peptide is shown in magenta; hGIPR Fab is shown as lavender and green surface for heavy (HC) and light (LC) chains, respectively; and GIPR ECD is shown in orange. (**G**) Insulin secretion in human islet microtissues treated with 2.8 mM glucose (closed circle), 11 mM glucose (closed square), or GIP + 11 mM glucose (open circles). (**I**) Insulin secretion in human islet microtissues after overnight incubation with hGIPR-Ab and then treated with 2.8 mM glucose (closed circle), 11 mM glucose (closed square), or 7 nM GIP + 11 mM glucose (open circles). Data represent means and SEM of $n = 4$ to 6 wells per treatment. (**H** and **J**) cAMP in cultured human subcutaneous adipocytes from three individual donors with human GIP (open circles) compared to basal (closed squares). (J) cAMP in cultured human subcutaneous adipocytes from three individual donors after overnight incubation with hGIPR-Ab and then treated with human 5 nM GIP (open circles) compared to 5 nM GIP only (closed circles) and basal (closed squares). Data represent means ± SEM of $n = 3$ donors with two to three wells per treatment per donor.

GIP is known to directly act on adipocytes (*10*). Transgenic rescue of adipocyte GIPR in GIPR KO mice restored HFD-induced body weight gain (*33*), and mice with adipocyte-specific GIPR KO are protected against DIO (*32*), suggesting a role for adipocyte GIPR in body weight regulation. Therefore, it is important to note that muGIPR-Ab treatment enhanced resting period lipid oxidation as determined by light cycle RER. Considering the sustained weight loss effects of muGIPR-Ab in $Gipr^{-/-\beta Cell}$ mice, adipocyte GIPR and its role in fatty acid metabolism may be central to our pharmacological findings.

In contrast to our findings using GIPR antagonists, Finan *et al.* (*34*) demonstrated that GIPR agonists also lead to weight loss, especially in combination with GLP-1R agonists because of reduced food intake. Although GIPR antagonism also reduced food intake, we additionally observed a direct effect on resting RER in DIO mice by muGIPR-Ab, consistent with the same observation in GIPR KO mice (*9*). A recent paper demonstrated that GIPR can become desensitized by GIP induction (*19*), which may provide a clue for the apparent discrepancy between our findings and those of Finan *et al.*

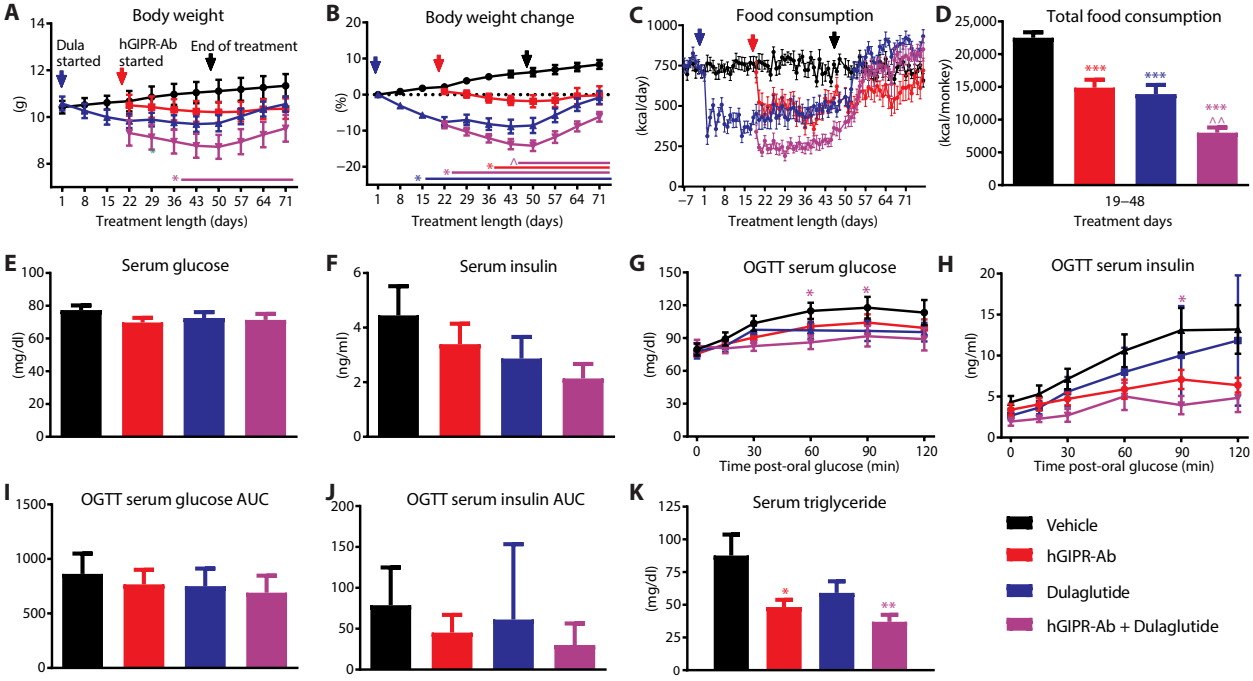

Fig. 7. hGIPR-Ab provides body weight loss alone and in combination with GLP-1R agonist dulaglutide in obese NHPs. Spontaneously obese naïve male NHPs were treated for 18 days either with vehicle or with dulaglutide every 3 days (in dose escalation regimen up to 0.25 mg/kg to circumvent nausea and vomiting associated with GLP-1R agonists). After 18 days, each group was further split into groups either with or without hGIPR-Ab (3 mg/kg every 6 days) for 30 additional days of treatment. After 48 days of treatment, all animals were monitored for an additional 28-day washout period ($n = 10$ NHPs per group). (**A**) Body weight was measured and used to calculate (**B**) percent change in body weight. (**C**) Food intake per animal (kcal/day) was measured daily and used to calculate (**D**) total food consumption during treatment days 19 to 48. Serum (**E**) glucose, (**F**) insulin, and (**K**) triglycerides were measured after an overnight fast on day 46. Posttreatment OGTT (4 g/kg) was performed on day 46. Serum (**G**) glucose and (**H**) insulin over the course of the OGTT were used to calculate the (**I**) glucose AUC and (**J**) insulin AUC. Data represent means ± SEM and were statistically assessed using (A, B, G, and H) repeated-measures two-way ANOVA with Sidak's test for multiple comparisons, (C) statistics not shown for simplicity, and (D to F and I to K) one-way ANOVA with Sidak's test for multiple comparisons. *$P < 0.05$, **$P < 0.01$, and ***$P < 0.001$ versus vehicle; ^$P < 0.05$ and ^^$P < 0.01$, dulaglutide versus hGIPR-Ab + dulaglutide.

Therefore, it is possible that GIPR activity is diminished by chronic GIPR agonism, thereby recapitulating the phenotypes associated with GIPR antagonism.

Our study has several limitations. First, we cannot conclude that GIPR antagonism in combination with GLP-1R agonists leads to greater weight loss than GLP-1R agonists alone because the GLP-1R agonists were not maximally dosed to establish the absolute maximum weight loss in our studies. Further, GIPR antagonism did not result in improved glucose tolerance, most likely because of reduced incretin function; however, the effects on glucose tolerance were not worsened, which is notable given the reduction in both fasting and postprandial serum insulin concentrations. The changes in insulin due to GIPR antagonism are expected to have beneficial effects on whole-body metabolism and are unlikely to have a negative impact on glucose homeostasis given the lack of impact on glucose tolerance. However, without a clamp study, we cannot address tissue-specific improvements in insulin sensitivity. Last, we note that the differences in pharmacological effects we observed in the murine and NHP obese models, most notably a minimal anorectic effect in mice and a more pronounced effect in the NHPs, are suggestive of species-specific differences in GIPR physiology. Currently, it is unclear which species is most translationally relevant to humans, but reproducible GWAS indicate that GIPR antagonism has a role in human obesity and BMI measures (*17*).

In conclusion, this study provides preclinical validation for a therapeutic approach to treat obesity and with anti-GIPR antibodies. This anti-obesity effect is independent of GIPR activity in β-cells. Further work must be done to understand the mechanism of action of these anti-GIPR antibodies and the role that GIPR antagonism plays on food intake, whether direct or indirect, as well as the site of action for anti-GIPR antibody alone and in combination with GLP-1R agonists.

MATERIALS AND METHODS

Study design

We identified and assessed muGIPR-Ab and hGIPR-Ab antibodies in vitro using recombinant cells expressing mouse, human, or NHP GIPR and assessed hGIPR-Ab in primary human adipocytes by measuring cAMP and in human pancreatic microtissues by measuring insulin secretion. For hGIPR-Ab, binding affinity was determined using KinExA measurements. Displacement studies using ^{125}I-GIP were performed to assess the mechanism of antagonism and confirmed by solving the crystal structure of the antibody with the human GIPR ECD. All animals were cared for in accordance with the Amgen Institutional Animal Care and Use Committee (IACUC) in Thousand Oaks, CA, and NHP studies were performed by Kunming Biomed International (KBI) in China. NHPs were housed in an Association for Assessment and Accreditation of Laboratory Animal Care (AAALAC)–accredited facility and all research protocols were reviewed, and the study was approved by KBI's IACUC. In vivo, DIO mice or obese NHPs were studied to assess PD, PK, and physiological

effects of the GIPR antibodies. Chronic dosing of either muGIPR-Ab or hGIPR-Ab alone or in combination with GLP-1R agonists was investigated, and body weight, food consumption, body composition, tissue weights, and glucose metabolism were measured. Calorimetry studies were conducted in metabolic cages to assess muGIPR-Ab treatment in DIO mice. Animals were randomized into groups of similar body weights before study initiation, and sample sizes were based on internal pilot study data. Investigators were not blinded for the mouse studies but were blinded for the NHP studies carried out by KBI in China. One NHP was excluded from the study because of very low food intake at the end of the dosing period, so treatment was ended early. Outliers were excluded from a group if the measurement was ±2 SDs from the group mean. The outcomes of all mouse studies and in vitro work presented have been replicated more than once.

Statistical analysis

One- or two-way ANOVA followed by Sidak's test for multiple comparisons (with repeated measures for time series data) was used in all studies, as noted in figure legends. For comparison between two groups, one-way ANOVA was performed. All tests used the software GraphPad Prism (GraphPad). Significance was defined as $^{*}P < 0.05$, $^{**}P < 0.01$, and $^{***}P < 0.001$.

SUPPLEMENTARY MATERIALS

www.sciencetranslationalmedicine.org/cgi/content/full/10/472/eaat3392/DC1
Materials and Methods
Fig. S1. PK-PD determination of muGIPR in vivo.
Fig. S2. muGIPR-Ab prevents weight gain in DIO mice.
Fig. S3. muGIPR-Ab enhances body weight loss in combination with the GLP-1R agonist liraglutide in DIO mice.
Fig. S4. muGIPR-Ab reduces insulin secretion after OGTT in DIO mice.
Fig. S5. muGIPR-Ab PK in DIO mice.
Fig. S6. The ability of muGIPR-Ab to prevent weight gain alone and to reduce body weight in combination with GLP-1R agonism is independent of pancreatic β-cell GIPR.
Fig. S7. Crystal structure of human GIPR ECD with hGIPR-Ab Fab.
Fig. S8. hGIPR-Ab PK in NHPs.
Table S1. Data collection and refinement statistics of hGIPR-Ab–ECD complex.
Table S2. Primary data.
References (*35*–*42*)

REFERENCES AND NOTES

1. M. A. Nauck, M. M. Heimesaat, C. Orskov, J. J. Holst, R. Ebert, W. Creutzfeldt, Preserved incretin activity of glucagon-like peptide 1 [7-36 amide] but not of synthetic human gastric inhibitory polypeptide in patients with type-2 diabetes mellitus. *J. Clin. Invest.* **91**, 301–307 (1993).
2. J. M. Falko, S. E. Crockett, S. Cataland, E. L. Mazzaferri, Gastric inhibitory polypeptide (GIP) stimulated by fat ingestion in man. *J. Clin. Endocrinol. Metab.* **41**, 260–265 (1975).
3. T. Vilsbøll, T. Krarup, J. Sonne, S. Madsbad, A. Volund, A. G. Juul, J. J. Holst, Incretin secretion in relation to meal size and body weight in healthy subjects and people with type 1 and type 2 diabetes mellitus. *J. Clin. Endocrinol. Metab.* **88**, 2706–2713 (2003).
4. W. Creutzfeldt, R. Ebert, B. Willms, H. Frerichs, J. C. Brown, Gastric inhibitory polypeptide (GIP) and insulin in obesity: Increased response to stimulation and defective feedback control of serum levels. *Diabetologia* **14**, 15–24 (1978).
5. T. Vilsbøll, T. Krarup, C. F. Deacon, S. Madsbad, J. J. Holst, Reduced postprandial concentrations of intact biologically active glucagon-like peptide 1 in type 2 diabetic patients. *Diabetes* **50**, 609–613 (2001).
6. K. Suzuki, N. Harada, S. Yamane, Y. Nakamura, K. Sasaki, D. Nasteska, E. Joo, K. Shibue, T. Harada, A. Hamasaki, K. Toyoda, K. Nagashima, N. Inagaki, Transcriptional regulatory factor X6 (Rfx6) increases gastric inhibitory polypeptide (GIP) expression in enteroendocrine K-cells and is involved in GIP hypersecretion in high fat diet-induced obesity. *J. Biol. Chem.* **288**, 1929–1938 (2013).
7. C. C. Tseng, L. A. Jarboe, M. M. Wolfe, Regulation of glucose-dependent insulinotropic peptide gene expression by a glucose meal. *Am. J. Physiol.* **266**, G887–G891 (1994).
8. C. Brøns, C. B. Jensen, H. Storgaard, N. J. Hiscock, A. White, J. S. Appel, S. Jacobsen, E. Nilsson, C. M. Larsen, A. Astrup, B. Quistorff, A. Vaag, Impact of short-term high-fat feeding on glucose and insulin metabolism in young healthy men. *J. Physiol.* **587**, 2387–2397 (2009).
9. K. Miyawaki, Y. Yamada, N. Ban, Y. Ihara, K. Tsukiyama, H. Zhou, S. Fujimoto, A. Oku, K. Tsuda, S. Toyokuni, H. Hiai, W. Mizunoya, T. Fushiki, J. J. Holst, M. Makino, A. Tashita, Y. Kobara, Y. Tsubamoto, T. Jinnouchi, T. Jomori, Y. Seino, Inhibition of gastric inhibitory polypeptide signaling prevents obesity. *Nat. Med.* **8**, 738–742 (2002).
10. R. G.-C. Yip, M. O. Boylan, T. J. Kieffer, M. M. Wolfe, Functional GIP receptors are present on adipocytes. *Endocrinology* **139**, 4004–4007 (1998).
11. B. Beck, J.-P. Max, Direct metabolic effects of gastric inhibitory polypeptide (GIP): Dissociation at physiological levels of effects on insulin-stimulated fatty acid and glucose incorporation in rat adipose tissue. *Diabetologia* **29**, 68 (1986).
12. S.-J. Kim, C. Nian, C. H. S. McIntosh, Activation of lipoprotein lipase by glucose-dependent insulinotropic polypeptide in adipocytes. A role for a protein kinase B, LKB1, and AMP-activated protein kinase cascade. *J. Biol. Chem.* **282**, 8557–8567 (2007).
13. B. Beck, J. P. Max, Hypersensitivity of adipose tissue to gastric inhibitory polypeptide action in the obese Zucker rat. *Cell. Mol. Biol.* **33**, 555–562 (1987).
14. H. Hauner, G. Glatting, D. Kaminska, E. F. Pfeiffer, Effects of gastric inhibitory polypeptide on glucose and lipid metabolism of isolated rat adipocytes. *Ann. Nutr. Metab.* **32**, 282–288 (1988).
15. J. M. E. Knapper, S. M. Puddicombe, L. M. Morgan, J. M. Fletcher, Investigations into the actions of glucose-dependent insulinotropic polypeptide and glucagon-like peptide-1(7–36)amide on lipoprotein lipase activity in explants of rat adipose tissue. *J. Nutr.* **125**, 183–188 (1995).
16. L. Getty-Kaushik, D. H. Song, M. O. Boylan, B. E. Corkey, M. M. Wolfe, Glucose-dependent insulinotropic polypeptide modulates adipocyte lipolysis and reesterification. *Obesity* **14**, 1124–1131 (2006).
17. S. I. Berndt, S. Gustafsson, R. Mägi, A. Ganna, E. Wheeler, M. F. Feitosa, A. E. Justice, K. L. Monda, D. C. Croteau-Chonka, F. R. Day, T. Esko, T. Fall, T. Ferreira, D. Gentilini, A. U. Jackson, J. Luan, J. C. Randall, S. Vedantam, C. J. Willer, T. W. Winkler, A. R. Wood, T. Workalemahu, Y.-J. Hu, S. H. Lee, L. Liang, D.-Y. Lin, J. L. Min, B. M. Neale, G. Thorleifsson, J. Yang, E. Albrecht, N. Amin, J. L. Bragg-Gresham, G. Cadby, M. den Heijer, N. Eklund, K. Fischer, A. Goel, J.-J. Hottenga, J. E. Huffman, I. Jarick, Å. Johansson, T. Johnson, S. Kanoni, M. E. Kleber, I. R. König, K. Kristiansson, Z. Kutalik, C. Lamina, C. Lecoeur, G. Li, M. Mangino, W. L. McArdle, C. Medina-Gomez, M. Müller-Nurasyid, J. S. Ngwa, I. M. Nolte, L. Paternoster, S. Pechlivanis, M. Perola, M. J. Peters, M. Preuss, L. M. Rose, J. Shi, D. Shungin, A. V. Smith, R. J. Strawbridge, I. Surakka, A. Teumer, M. D. Trip, J. Tyrer, J. V. Van Vliet-Ostaptchouk, L. Vandenput, L. L. Waite, J. H. Zhao, D. Absher, F. W. Asselbergs, M. Atalay, A. P. Attwood, A. J. Balmforth, H. Basart, J. Beilby, L. L. Bonnycastle, P. Brambilla, M. Bruinenberg, H. Campbell, D. I. Chasman, P. S. Chines, F. S. Collins, J. M. Connell, W. O. Cookson, U. de Faire, F. de Vegt, M. Dei, M. Dimitriou, S. Edkins, K. Estrada, D. M. Evans, M. Farrall, M. M. Ferrario, J. Ferrières, L. Franke, F. Frau, P. V. Gejman, H. Grallert, H. Gronberg, V. Gudnason, A. S. Hall, P. Hall, A.-L. Hartikainen, C. Hayward, N. L. Heard-Costa, A. C. Heath, J. Hebebrand, G. Homuth, F. B. Hu, S. E. Hunt, E. Hyppönen, C. Iribarren, K. B. Jacobs, J.-O. Jansson, A. Jula, M. Kähönen, S. Kathiresan, F. Kee, K.-T. Khaw, M. Kivimäki, W. Koenig, A. T. Kraja, M. Kumari, K. Kuulasmaa, J. Kuusisto, J. H. Laitinen, T. A. Lakka, C. Langenberg, L. J. Launer, L. Lind, J. Lindström, J. Liu, A. Liuzzi, M.-L. Lokki, M. Lorentzon, P. A. Madden, P. K. Magnusson, P. Manunta, D. Marek, W. März, I. Mateo Leach, B. McKnight, S. E. Medland, E. Mihailov, L. Milani, G. W. Montgomery, V. Mooser, T. W. Mühleisen, P. B. Munroe, A. W. Musk, N. Narisu, G. Navis, G. Nicholson, E. A. Nohr, K. K. Ong, B. A. Oostra, C. N. Palmer, A. Palotie, J. F. Peden, N. Pedersen, A. Peters, O. Polasek, A. Pouta, P. P. Pramstaller, I. Prokopenko, C. Pütter, A. Radhakrishnan, O. Raitakari, A. Rendon, F. Rivadeneira, I. Rudan, T. E. Saaristo, J. G. Sambrook, A. R. Sanders, S. Sanna, J. Saramies, S. Schipf, S. Schreiber, H. Schunkert, S.-Y. Shin, S. Signorini, J. Sinisalo, B. Skrobek, N. Soranzo, A. Stančáková, K. Stark, J. C. Stephens, K. Stirrups, R. P. Stolk, M. Stumvoll, A. J. Swift, E. V. Theodoraki, B. Thorand, D.-A. Tregouet, E. Tremoli, M. M. Van der Klauw, J. B. J. van Meurs, S. H. Vermeulen, J. Viikari, J. Virtamo, V. Vitart, G. Waeber, Z. Wang, E. Widén, S. H. Wild, G. Willemsen, B. R. Winkelmann, J. C. M. Witteman, B. H. R. Wolffenbuttel, A. Wong, A. F. Wright, M. C. Zillikens, P. Amouyel, B. O. Boehm, E. Boerwinkle, D. I. Boomsma, M. J. Caulfield, S. J. Chanock, L. A. Cupples, D. Cusi, G. V. Dedoussis, J. Erdmann, J. G. Eriksson, P. W. Franks, P. Froguel, C. Gieger, U. Gyllensten, A. Hamsten, T. B. Harris, C. Hengstenberg, A. A. Hicks, A. Hingorani, A. Hinney, A. Hofman, K. G. Hovingh, K. Hveem, T. Illig, M.-R. Jarvelin, K.-H. Jöckel, S. M. Keinanen-Kiukaanniemi, L. A. Kiemeney, D. Kuh, M. Laakso, T. Lehtimäki, D. F. Levinson, N. G. Martin, A. Metspalu, A. D. Morris, M. S. Nieminen, I. Njølstad, C. Ohlsson, A. J. Oldehinkel, W. H. Ouwehand, L. J. Palmer, B. Penninx, C. Power, M. A. Province, B. M. Psaty, L. Qi, R. Rauramaa, P. M. Ridker, S. Ripatti, V. Salomaa, N. J. Samani, H. Snieder, T. I. A. Sørensen, T. D. Spector, K. Stefansson, A. Tönjes, J. Tuomilehto, A. G. Uitterlinden, M. Uusitupa, P. van der Harst, P. Vollenweider, H. Wallaschofski, N. J. Wareham, H. Watkins, H.-E. Wichmann, J. F. Wilson, G. R. Abecasis, T. L. Assimes, I. Barroso, M. Boehnke, I. B. Borecki, P. Deloukas, C. S. Fox, T. Frayling, L. C. Groop, T. Haritunian, I. M. Heid, D. Hunter, R. C. Kaplan, F. Karpe, M. F. Moffatt, K. L. Mohlke, J. R. O'Connell, Y. Pawitan, E. E. Schadt, D. Schlessinger, V. Steinthorsdottir,

D. P. Strachan, U. Thorsteinsdottir, C. M. van Duijn, P. M. Visscher, A. M. Di Blasio, J. N. Hirschhorn, C. M. Lindgren, A. P. Morris, D. Meyre, A. Scherag, M. I. McCarthy, E. K. Speliotes, K. E. North, R. J. F. Loos, E. Ingelsson, Genome-wide meta-analysis identifies 11 new loci for anthropometric traits and provides insights into genetic architecture. *Nat. Genet.* **45**, 501–512 (2013).
18. K. Almind, L. Ambye, S. A. Urhammer, T. Hansen, S. M. Echwald, J. J. Holst, J. Gromada, B. Thorens, O. Pedersen, Discovery of amino acid variants in the human glucose-dependent insulinotropic polypeptide (GIP) receptor: The impact on the pancreatic beta cell responses and functional expression studies in Chinese hamster fibroblast cells. *Diabetologia* **41**, 1194–1198 (1998).
19. S. Mohammad, R. T. Patel, J. Bruno, M. S. Panhwar, J. Wen, T. E. McGraw, A naturally occurring GIP receptor variant undergoes enhanced agonist-induced desensitization, which impairs GIP control of adipose insulin sensitivity. *Mol. Cell. Biol.* **34**, 3618–3629 (2014).
20. M. C. Althage, E. L. Ford, S. Wang, P. Tso, K. S. Polonsky, B. M. Wice, Targeted ablation of glucose-dependent insulinotropic polypeptide-producing cells in transgenic mice reduces obesity and insulin resistance induced by a high fat diet. *J. Biol. Chem.* **283**, 18365–18376 (2008).
21. D. Nasteska, N. Harada, K. Suzuki, S. Yamane, A. Hamasaki, E. Joo, K. Iwasaki, K. Shibue, T. Harada, N. Inagaki, Chronic reduction of GIP secretion alleviates obesity and insulin resistance under high-fat diet conditions. *Diabetes* **63**, 2332–2343 (2014).
22. J. E. Campbell, J. R. Ussher, E. E. Mulvihill, J. Kolic, L. L. Baggio, X. Cao, Y. Liu, B. J. Lamont, T. Morii, C. J. Streutker, N. Tamarina, L. H. Philipson, J. L. Wrana, P. E. MacDonald, D. J. Drucker, TCF1 links GIPR signaling to the control of beta cell function and survival. *Nat. Med.* **22**, 84–90 (2016).
23. C. Postic, M. A. Magnuson, Role of glucokinase (GK) in the maintenance of glucose homeostasis. Specific disruption of the gene by the Cre-loxP technique. *Journ. Annu. Diabetol. Hotel Dieu* 115–124 (1999).
24. R. A. Pederson, J. C. Brown, Interaction of gastric inhibitory polypeptide, glucose, and arginine on insulin and glucagon secretion from the perfused rat pancreas. *Endocrinology* **103**, 610–615 (1978).
25. J. J. Meier, B. Gallwitz, N. Siepmann, J. J. Holst, C. F. Deacon, W. E. Schmidt, M. A. Nauck, Gastric inhibitory polypeptide (GIP) dose-dependently stimulates glucagon secretion in healthy human subjects at euglycaemia. *Diabetologia* **46**, 798–801 (2003).
26. C. M. Koth, J. M. Murray, S. Mukund, A. Madjidi, A. Minn, H. J. Clarke, T. Wong, V. Chiang, E. Luis, A. Estevez, J. Rondon, Y. Zhang, I. Hötzel, B. B. Allan, Molecular basis for negative regulation of the glucagon receptor. *Proc. Natl. Acad. Sci. U.S.A.* **109**, 14393–14398 (2012).
27. C. Parthier, M. Kleinschmidt, P. Neumann, R. Rudolph, S. Manhart, D. Schlenzig, J. Fanghänel, J.-U. Rahfeld, H.-U. Demuth, M. T. Stubbs, Crystal structure of the incretin-bound extracellular domain of a G protein-coupled receptor. *Proc. Natl. Acad. Sci. U.S.A.* **104**, 13942–13947 (2007).
28. C. R. Underwood, P. Garibay, L. B. Knudsen, S. Hastrup, G. H. Peters, R. Rudolph, S. Reedtz-Runge, Crystal structure of glucagon-like peptide-1 in complex with the extracellular domain of the glucagon-like peptide-1 receptor. *J. Biol. Chem.* **285**, 723–730 (2009).
29. T. B. Usdin, E. Mezey, D. C. Button, M. J. Brownstein, T. I. Bonner, Gastric inhibitory polypeptide receptor, a member of the secretin-vasoactive intestinal peptide receptor family, is widely distributed in peripheral organs and the brain. *Endocrinology* **133**, 2861–2870 (1993).
30. P. Ravn, C. Madhurantakam, S. Kunze, E. Matthews, C. Priest, S. O'Brien, A. Collinson, M. Papworth, M. Fritsch-Fredin, L. Jermutus, L. Benthem, M. Gruetter, R. H. Jackson, Structural and pharmacological characterization of novel potent and selective monoclonal antibody antagonists of glucose-dependent insulinotropic polypeptide receptor. *J. Biol. Chem.* **288**, 19760–19772 (2013).
31. M. O. Boylan, P. A. Glazebrook, M. Tatalovic, M. M. Wolfe, Gastric inhibitory polypeptide immunoneutralization attenuates development of obesity in mice. *Am. J. Physiol. Endocrinol. Metab.* **309**, E1008–E1018 (2015).
32. E. Joo, N. Harada, S. Yamane, T. Fukushima, D. Taura, K. Iwasaki, A. Sankoda, K. Shibue, T. Harada, K. Suzuki, A. Hamasaki, N. Inagaki, Inhibition of gastric inhibitory polypeptide receptor signaling in adipose tissue reduces insulin resistance and hepatic steatosis in high-fat diet-fed mice. *Diabetes* **66**, 868–879 (2017).
33. R. Ugleholdt, J. Pedersen, M. R. Bassi, E.-M. Füchtbauer, S. M. Jørgensen, H.-L. Kissow, N. Nytofte, S. S. Poulsen, M. M. Rosenkilde, Y. Seino, P. Thams, P. J. Holst, J. J. Holst, Transgenic rescue of adipocyte glucose-dependent insulinotropic polypeptide receptor expression restores high fat diet-induced body weight gain. *J. Biol. Chem.* **286**, 44632–44645 (2011).
34. B. Finan, T. Ma, N. Ottaway, T. D. Müller, K. M. Habegger, K. M. Heppner, H. Kirchner, J. Holland, J. Hembree, C. Raver, S. H. Lockie, D. L. Smiley, V. Gelfanov, B. Yang, S. Hofmann, D. Bruemmer, D. J. Drucker, P. T. Pfluger, D. Perez-Tilve, J. Gidda, L. Vignati, L. Zhang, J. B. Hauptman, M. Lau, M. Brecheisen, S. Uhles, W. Riboulet, E. Hainaut, E. Sebokova, K. Conde-Knape, A. Konkar, R. D. DiMarchi, M. H. Tschop, Unimolecular dual incretins maximize metabolic benefits in rodents, monkeys, and humans. *Sci. Transl. Med.* **5**, 209ra151 (2013).
35. C. Postic, M. Shiota, K. D. Niswender, T. L. Jetton, Y. Chen, J. M. Moates, K. D. Shelton, J. Lindner, A. D. Cherrington, M. A. Magnuson, Dual roles for glucokinase in glucose homeostasis as determined by liver and pancreatic β cell-specific gene knock-outs using Cre recombinase. *J. Biol. Chem.* **274**, 305–315 (1999).
36. W. Kabsch, XDS. *Acta Crystallogr. D Biol. Crystallogr.* **66**, 125–132 (2010).
37. P. R. Evans, G. N. Murshudov, How good are my data and what is the resolution? *Acta Crystallogr. D Biol. Crystallogr.* **69**, 1204–1214 (2013).
38. Collaborative Computational Project, Number 4, The CCP4 suite: Programs for protein crystallography. *Acta Crystallogr. D Biol. Crystallogr.* **50**, 760–763 (1994).
39. A. J. McCoy, R. W. Grosse-Kunstleve, P. D. Adams, M. D. Winn, L. C. Storoni, R. J. Read, *Phaser* crystallographic software. *J. Appl. Cryst.* **40**, 658–674 (2007).
40. G. N. Murshudov, A. A. Vagin, E. J. Dodson, Refinement of macromolecular structures by the maximum-likelihood method. *Acta Crystallogr. D Biol. Crystallogr.* **53**, 240–255 (1997).
41. P. D. Adams, P. V. Afonine, G. Bunkóczi, V. B. Chen, I. W. Davis, N. Echols, J. J. Headd, L.-W. Hung, G. J. Kapral, R. W. Grosse-Kunstleve, A. J. McCoy, N. W. Moriarty, R. Oeffner, R. J. Read, D. C. Richardson, J. S. Richardson, T. C. Terwilliger, P. H. Zwart, *Phenix*: A comprehensive python-based system for macromolecular structure solution. *Acta Crystallogr. D Biol. Crystallogr.* **66**, 213–221 (2010).
42. P. Emsley, K. Cowtan, *Coot*: Model-building tools for molecular graphics. *Acta Crystallogr. D Biol. Crystallogr.* **60**, 2126–2132 (2004).

Acknowledgments: We would like to thank the Biologics Team (Amgen) for production of proteins and H. Li and L. Tran (PKDM, Amgen) for measuring antibody exposure. **Funding:** Amgen Inc. funded all work presented. Crystallography datasets were collected at the Advanced Light Source, Lawrence Berkeley National Laboratory. The Berkeley Center for Structural Biology is supported, in part, by the NIH, the National Institute of General Medical Sciences, and the Howard Hughes Medical Institute. The Advanced Light Source is supported by the Director, Office of Science, and Office of Basic Energy Sciences of the U.S. Department of Energy under contract no. DE-AC02-05CH11231. **Author contributions:** E.A.K., J.W., J.Y., M.M.V., and D.J.L. conceptualized and designed studies. S.D.-H.S., D.B., S.A.T., C.M.A., T.M., B.C., C.M.M., and I.N.F. generated cell lines and protein reagents or identified antibodies. E.A.K., J.W., J.Y., X.M., R.K., T.H., L.D., L.A., S.-C.L., R.J.M.K., G.S., J.L., Q.C., Z.W., J.B.R., and C.H. conducted experiments and provided data. E.A.K., J.W., and D.J.L. wrote the manuscript. **Competing interests:** All authors are or were employees of Amgen Inc. and have received Amgen stock. Most of the work has been included in a patent: PCT/US2016/068138, "Method of treating or ameliorating metabolic disorders using binding proteins for gastric inhibitory peptide receptor (GIPR) in combination with GLP-1 agonists." **Data and materials availability:** All data associated with this study can be found in the paper or the Supplementary Materials. The crystal structure of the human GIPR ECD with hGIPR-Ab Fab is available at the PDB, code 6DKJ (www.rcsb.org/). Reagents can be provided by and at Amgen's sole discretion pending scientific review and a completed material transfer agreement with Amgen. Requests from an academic or nonprofit institution should be submitted at wwwext.amgen.com/partners/academic-collaborations/new-requests/. Requests from a for-profit entity should be submitted to BDopportunities@amgen.com.

Submitted 16 February 2018
Resubmitted 12 September 2018
Accepted 30 November 2018
Published 19 December 2018
10.1126/scitranslmed.aat3392

Citation: E. A. Killion, J. Wang, J. Yie, S. D.-H. Shi, D. Bates, X. Min, R. Komorowski, T. Hager, L. Deng, L. Atangan, S.-C. Lu, R. J. M. Kurzeja, G. Sivits, J. Lin, Q. Chen, Z. Wang, S. A. Thibault, C. M. Abbott, T. Meng, B. Clavette, C. M. Murawsky, I. N. Foltz, J. B. Rottman, C. Hale, M. M. Véniant, D. J. Lloyd, Anti-obesity effects of GIPR antagonists alone and in combination with GLP-1R agonists in preclinical models. *Sci. Transl. Med.* **10**, eaat3392 (2018).

Science Translational Medicine

Anti-obesity effects of GIPR antagonists alone and in combination with GLP-1R agonists in preclinical models

Elizabeth A. Killion, Jinghong Wang, Junming Yie, Stone D.-H. Shi, Darren Bates, Xiaoshan Min, Renee Komorowski, Todd Hager, Liying Deng, Larissa Atangan, Shu-Chen Lu, Robert J. M. Kurzeja, Glenn Sivits, Joanne Lin, Qing Chen, Zhulun Wang, Stephen A. Thibault, Christina M. Abbott, Tina Meng, Brandon Clavette, Christopher M. Murawsky, Ian N. Foltz, James B. Rottman, Clarence Hale, Murielle M. Véniant and David J. Lloyd

Sci Transl Med **10**, eaat3392.
DOI: 10.1126/scitranslmed.aat3392

Win one for the GIPR

Glucose-dependent insulinotropic polypeptide (GIP), secreted by the gut to help stimulate insulin release, is a promising therapeutic target in obesity. Here, Killion *et al.* developed an antibody-based strategy to target the GIP receptor (GIPR) to block the action of GIP. GIPR-Ab treatment of obese mice and nonhuman primates elicited improvements in body weight and fat mass, and also improved fasting serum insulin and triglycerides but not glucose tolerance. Combination with glucagon-like peptide-1 receptor (GLP-1R) agonists further enhanced weight loss. These studies suggest that antagonistic GIPR antibodies are promising candidates for obesity treatment meriting further study.